ISSN 1990-7931, Russian Journal of Physical Chemistry B, 2020, Vol. 14, No. 4, pp. 705–713. © Pleiades Publishing, Ltd., 2020.
Russian Text © The Author(s), 2020, published in Khimicheskaya Fizika, 2020, Vol. 39, No. 7, pp. 72–81.

CHEMICAL PHYSICS OF NANOMATERIALS

Molecular Dynamic Behavior of Lithium Atoms in a Flat Silicene Pore on a Copper Substrate

A. E. Galashev[a, b, *], O. R. Rakhmanova[a, b], and A. V. Isakov[a]

[a] *Institute of High-Temperature Electrochemistry, Ural Branch, Russian Academy of Sciences, Yekaterinburg, 620137 Russia*
[b] *Yeltsin Ural Federal University, Yekaterinburg, 620002 Russia*
**e-mail: alexander-galashev@yandex.ru*

Received May 13, 2019; revised July 11, 2019; accepted July 22, 2019

Abstract—The processes of lithization/delithization in a flat slit-like pore formed from defective silicene sheets and located on a copper substrate are considered in a molecular dynamic (MD) simulation. Depending on the type of the defects (mono-, bi-, tri-, hexavacancies), such a pore can hold up to 67, 86, 60, and 23 lithium atoms during the entire MD calculation with the duration of up to 1 ns without being destroyed. As a result of the intercalation/deintercalation cycle, the structure of defective silicene changes, especially in the presence of tri- and hexavacancies. With the increase in the size of the defects, the mobility of the lithium atoms in the silicene pore also increases. The shape of the silicene sheets is not restored after delithization, and the volume of the space enclosed between them slightly changes. Effective use of silicene in lithium-ion batteries assumes that only mono- and bivacancies are present in its sheets.

Keywords: molecular dynamics, silicene, copper substrate, lithization, delithization, mobility coefficient
DOI: 10.1134/S1990793120040053

INTRODUCTION

The use of batteries with a high energy density, long lifetime, and low cost is a key factor for consumer electronics, electric cars, and energy storage in grids [1–3]. The operation of lithium-ion batteries is based on the phenomenon of intercalation of lithium into the material of the electrode. Upon the charging of a battery, lithium is extracted from the material of the positive electrode and it is intercalated into the material of the negative electrode most often fabricated from graphite. Upon its discharge, these processes are reversed. One of the main characteristics of an electrode is its intercalation capacity, determined as the quantity of electricity imparted to the electrode upon full charging and calculated per the unit mass or volume. In particular, in the case of the full charging of a carbon electrode, the intercalation capacity is 372 mA h g^{-1}. For a silicon electrode, this characteristic has a value of 4200 mA h g^{-1} [4]. The rate of the intercalation/deintercalation reaction is determined by the rate of diffusion of lithium in the solid phase. The coefficient of diffusion of lithium in the process of lithization/delithization, e.g., in bilayer graphene at room temperature, is 7×10^{-5} cm^2/s [5]. To avoid a significant change in the volume (almost fourfold in the case of the use of crystalline silicon) during the intercalation of lithium, it is proposed to use negative electrodes made of thin-film materials [6–10]. Autonomous bilayer silicene does not undergo significant structural changes during the cycles of lithization/delithization, while the change in the volume is not more than 25%, and the energy barrier for the diffusion of lithium is quite low (<0.6 eV) [11]. The silicene found on a copper substrate is an *n*-type semiconductor. In this case, the hybridization between the two-dimensional structure and substrate is so strong that the Dirac cone in the band structure of silicene disappears [12]. However, Dirac fermions can be recovered in the case of the intercalation of alkaline metal atoms into the system. There is quite a lot of data on the properties of silicene located on a silver substrate [7, 13, 14]; however, other substrate materials still remain unfamiliar. Copper is the most widely used metal in electrochemical instruments. It has a relatively low cost and is abundant in the Earth's crust (compared to silver). The experiment [15] and molecular dynamic (MD) studies [16] suggest the formation of an amorphous structure at the Cu/Si(001) boundary of two bulk phases, and mutual diffusion may reach a depth of 10 nm depending on the temperature of the substrate [17]. The properties of silicene located on a Cu substrate are still understudied.

This paper aims to study the molecular dynamics of the behavior of the functionalized bilayer silicene located on a copper substrate during the processes of lithization/delithization, determine the kinetic and dynamic properties of the system, and assess the possibility of its application as the anode of a lithium-ion battery.

THE MOLECULAR DYNAMIC MODEL

We chose the Tersoff potential model [18] with the parameters from the work [19] as the multibody potential of the interaction of silicon atoms in silicene. The embedded atom method (EAM) was used to describe the interatomic interactions in the copper substrate [20]. The Morse potential with the parameters from the works [21–23] and the parameters calculated through interpolation correlations [4] was applied between the Cu–Si, Si–Si (belonging to different sheets), Cu–Li, Si–Li, and Li–Li pairs.

The model of silicene under consideration is a reconstruction of a 4 × 4 surface. The unit cell contains 18 Si atoms located in the form of a rhomb. Six of them are displaced to a distance of 0.074 nm perpendicularly to the surface, upwards for the upper silicene sheet, and downwards, for the lower silicene sheet. A flat slit-like pore (SP) formed by two silicene sheets located on a Cu(111) substrate was modeled. The value of the pore gap h_g (distance between the sheets) was 0.75 nm. The earlier calculations on the investigation of the behavior of a lithium ion in a silicene pore [6] showed that Li^+ entering the pore can be held in it for at least 100 ps while interacting with the pore walls at this particular gap.

The silicene sheets had a rectangular shape with a size of 4.7 × 4.0 nm. In the case of the presence of a perfect structure, they contained 300 Si atoms each. Defects of various sizes were generated in the silicene: 1, 2, 3, and 6 silicon atoms each were removed in 9 places approximately uniformly distributed over the surface of the sheets, and mono-, bi-, tri-, and hexavacancies were thus formed. The experimental data indicate the presence of defects in silicene irrespective of the substrate used for its preparation [24].

Bilayer silicene was located in accordance with the Bernal stacking (*ABAB*...) on a fixed Cu(111) substrate that interacts with the silicene. Fixing the edges of the silicene sheets makes it possible to avoid their nonphysical turns related to the presence of uncompensated local rotary momenta [1, 2]. The distance r_{Cu-Si} between the lower silicene sheet and metallic substrate calculated according to the density functional theory is 0.2481 nm [25]. However, the preliminary calculations with the use of such a value of the gap between the silicene sheets showed continuous distancing of the latter from the copper substrate during the intercalation of lithium. Because of this, the value of r_{Cu-Si} was increased to 0.27 nm, which corresponds to the data of the work [26]. The MD calculations of all the systems were performed in the NVT ensemble at 300 K.

To prevent strong buckling of silicene sheets in the center of the SP, two six-membered cyclic formations were vertically placed between them at an equal distance (in the form of a column), in the nodes of which Si atoms were located. This stabilizing structure was immobile; however, it interacted with the Li and Si atoms by the Morse potential [22, 23]. The modeling of the filling of the initially hollow silicene SP located on the copper substrate showed the appearance of significant caving of the silicene sheets [7]. The insertion of a vertical stabilizing support between the silicene sheets made it possible to avoid this [27]. The insertion of the "column" into the SP resulted in the decrease in the deformation of the silicene sheets, especially those containing large vacancy-type defects. This made it possible to make the filling of the SP with lithium more significant. The fillability of the pore decreased by 20–30% in the absence of the "column."

The process of lithization of bilayer silicene on the substrate was executed by the periodic pairwise addition of lithium ions into the system. The original position of a pair of Li^+ ions was randomly selected on a line parallel to the y axis and located near the pore entrance at the level $h_g/2$. A procedure of relaxation of the system for 200 ps was preliminarily performed prior to the implementation of the process of intercalation. Then the lithium ions were brought into the SP over time intervals of 10 ps or $10^5\Delta t$, where $\Delta t = 1 \times 10^{-16}$ s is the value of the time step. It was experimentally found that, during the intercalation, the Li^+ ion quickly acquires an electron and becomes a neutral atom on penetrating into the anode [28]. During the reverse process (deintercalation), Li atoms lose electrons and rush to the cathode in the form of ions. Such a recharge always occurs in silicon but does not occur in carbon-based materials (e.g., graphite). The duration of the calculation of 10 ps is sufficient to calculate the equilibrium properties of the system (full energy and stress tensor) and mobility coefficients of the atoms. In addition, the ions can find energetically favorable places in the SP and stay in them with a high degree of probability on such an interval.

An electric field with a value of 10^3 V/m had an electric field strength vector directed along the x axis. The charges (ions) moved along the pore under the action of this electric field with the Coulomb repulsion relative to each other. After 10 ps, these ions that filled the SP became atoms and further remained electrically neutral during the intercalation. A new ion pair was launched every 10 ps. Such a temporal interval was sufficient for the calculation of the stress tensor of silicene and the mobility coefficient of the Li atoms. The process of intercalation stopped when the system started destroying (in the case of the presence of hexavacancies) or the lithium ions and atoms started leaving actively the SP. For example, the process of filling a silicene pore formed from the sheets with monovacancies with lithium lasted for 0.75 ns. In addition to the visual observation of the system, a jump in the total energy of the system served as the indicator of the filling of the SP.

The process of delithization in the reverse direction occurred by the pairwise removal of the lithium ions from the pore. After removing the Li^+ ions that had

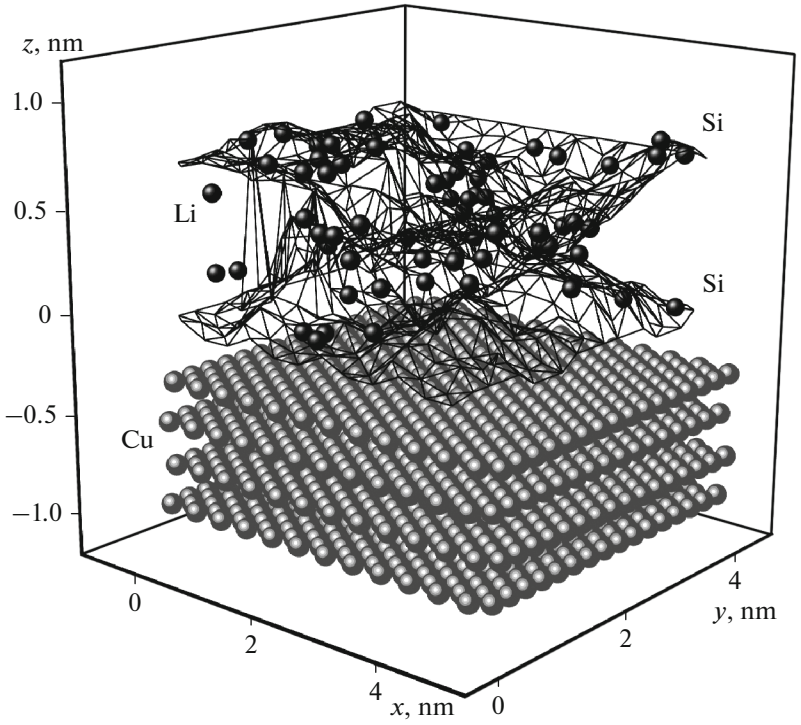

Fig. 1. Slit-like pore formed by silicene sheets with monovacancies and located on a Cu(111) substrate after the intercalation of lithium.

already left the pore at the previous stage from consideration, a new ion pair started moving under the action of an electric field with the value of 10^5 V/m directed in the reverse direction along the x axis. The intensity of the electric field maintaining the process of deintercalation was increased so that the ions overcame the energy barrier related to their exit from the SP. The time of observation of the system was increased up to 200000 time steps in this case. The codes of the LAMMPS software complex [29] modified by us, which was operated on an URAN hybrid cluster-type computer at the Krasovskii Institute of Mathematics and Mechanics, Ural Branch, Russian Academy of Sciences were used in the calculations.

The mobility coefficient D of the lithium atoms in the SP was calculated through the mean square displacement of the atoms $\left\langle\left[\Delta\mathbf{r}(t)\right]^2\right\rangle$:

$$D = \lim_{t\to\infty}\frac{1}{2\Gamma t}\left\langle\left[\Delta\mathbf{r}(t)\right]^2\right\rangle_{t_0}. \quad (1)$$

Here, $\Gamma = 3$ is the dimensionality of the space. $\langle\ldots\rangle_{t_0}$ denotes averaging by the initial time moments.

To calculate the stresses appearing in the silicene, the sheets were divided into surface elements. The stresses $\sigma_{u\alpha}(l)$ appearing in the direction of action of the forces $\alpha = x, y$, and z are calculated on each element with number l, which has the orientation along $u = x, y, x$. The products of the projections of the velocities of atoms and projections of forces f_{ij}^{α} acting on the l-element from the side of other atoms while observing the corresponding conditions [30] are used in these calculations:

$$\sigma_{u\alpha}(l) = \left\langle\sum_i^k\frac{1}{\Omega}\left(mv_u^i v_\alpha^i\right)\right\rangle + \frac{1}{S_l}\left\langle\sum_i^k\sum_{j\neq i}^{(u_i\le u, u_j\ge u)}\left(f_{ij}^{\alpha}\right)\right\rangle. \quad (2)$$

Here, k is the number of atoms on the l-element, Ω is the volume per atom, m is the atomic mass, v_α^i is the α projection of the velocity of the ith atom, and S_l is the area of the l-element. The conditions of summation over j in the last sum of expression (2) are shown in both the lower and upper indices of the sum; the force appearing upon the interaction of atoms i and j passes through the l-element; u_i is the current coordinate of atom i; the upper index u of the sum denotes the coordinate of the point of intersection of the straight line passing through the centers of atoms i and j with the l-element.

RESULTS AND DISCUSSION

A silicene SP located on a Cu(111) substrate after full intercalation with lithium is depicted in Fig. 1 in the form of a tenuous web to show all the Li atoms deposited onto the pore walls. It is seen that the arrangement of the Li atoms in the pore is nonuniform. The first half of the pore along the direction of

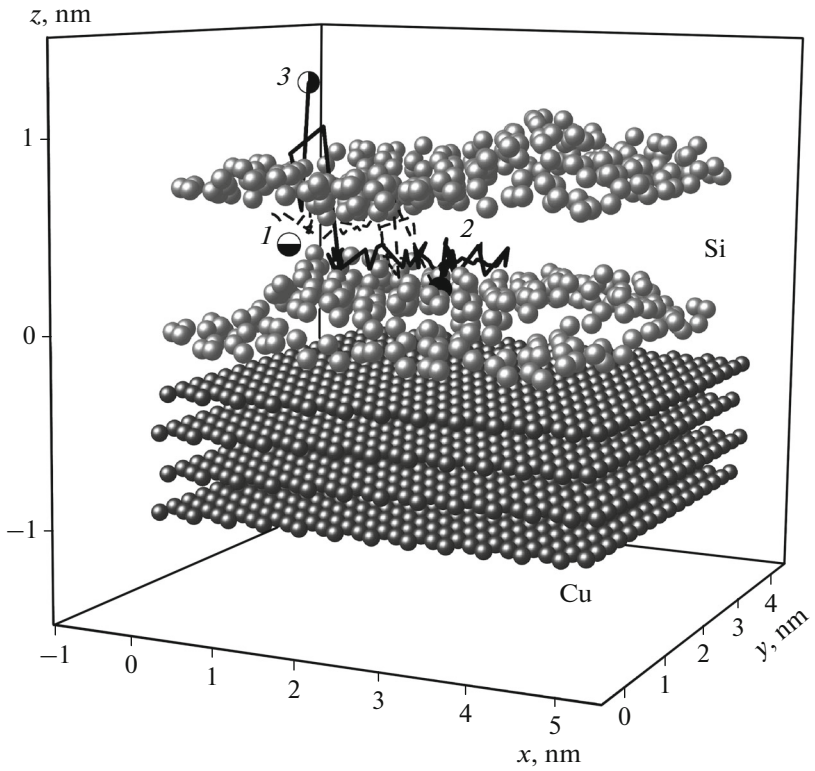

Fig. 2. Trajectory of the movement of a lithium ion in the process of lithization (the dashed line) and delithization (the solid line) in a silicene SP containing trivacancies on a Cu(111) substrate: (*1*) initial point of the trajectory of the ion (before the entrance to the channel) at $t = 0$ ps, (*2*) final point of the trajectory of the ion after lithization, and (*3*) final point of the trajectory of the ion after delithization.

the x axis is filled with Li atoms significantly denser that the second half: 33 Li atoms have coordinate $x \le 2.6$ nm, and just 15 Li atoms are arranged in the space with coordinate $x > 2.6$ nm. A convexity in relation to the substrate is observed in the middle part of the lower silicene sheet, while concavity is observed in the same part of the upper sheet. The significant narrowing of the pore in the middle part complicates its passage by Li^+ ions and limits the fillability of the pore with lithium.

The trajectory of the movement of a lithium ion in a slit-like pore (the sheets of which are filled with trivacancies) in the process of lithization (the dashed line) and delithization (the solid line) is shown in Fig. 2. Numbers *1*, *2*, and *3* denote the points of entrance of the ion into the pore, fixation of the ion in the SP after lithization, and exit of the ion from the pore after delithization, respectively. Over the time of lithization (10 ps), the ion manages to overcome the entry barrier to the SP [6], move forward inside the pore to a distance equal to about half of the length of the SP (~2.5 nm), and become fixed in the "saddle" point, most often, over the center of the six-membered Si ring. Upon further lithization, an Li atom can at this point make small vibrational motions in the vicinity of the point of fixation in the pore. During delithization, on acquiring a charge again, the lithium ion starts moving in the direction of the field towards the exit from the pore and manages to leave the SP in 20 ps. It should be noted that a correlation between the size of the vacancy defects in the silicene sheets and the rate of delithization of the SP is observed; thus, the larger the vacancy the faster the lithium ion leaves the slit-like pore.

Table 1. Maximum number of the lithium atoms held in a silicene SP containing different types of vacancies and located on silver and copper substrates

Type of the vacancies in the silicene sheets	Type of the substrate	
	silver	copper
Perfect	39	48
Monovacancies	51	67
Bivacancies	71	86
Trivacancies	79	60
Hexavacancies	42	23

The maximum number of Li atoms intercalated into silicene SPs with different types of vacancy defects is presented in Table 1. For comparison, it also presents the results of the intercalation of lithium in

the case when an SP is on an Ag(111) substrate in the absence of a "column" between the silicene sheets. It is seen that, in the cases suitable for real use, i.e., for perfect silicene and silicene with mono- and bivacancies, the number of the Li atoms intercalated into the pore is noticeably higher when the silicene sheets lie on a silver substrate. The calculations for the pores with tri- and hexavacancies showed the inviability of these structures due to the significant structural rearrangements in silicene and the initiation of the destruction of its sheets.

Let us consider the behavior of the defects and belonging of Li atoms to silicene sheets in more detail by way of example of a silicene pore with monovacancies fully filled with lithium. The configurations under study refers to the time point 0.75 ns (or $7.5 \times 10^6 \Delta t$). The *xy* projections of the (a) upper and (b) lower layers of the pore divided by the central plane ($z = h_g/2$) are shown in Fig. 3 (the view from the side of the $z = h_g/2$ plane). One of the monovacancies of the lower sheet was transformed to a large hollow formation, which is apparently a demonstration of the destructive action of the copper substrate on silicene. The transformation of some monovacancies to cyclic oval-shaped formations containing from seven to nine Si atoms is observed in the upper sheet. The eight monovacancies of the lower sheet and seven monovacancies of the upper sheet became deformed but retained their initial shape. The upper and lower parts of the pore have equal volumes; however, the number of Li atoms in them is different; thus, 37 atoms are present in the upper part and 30 atoms are present in the lower part. The lithium atoms present in the SP are predominantly located over the centers of the six-membered silicon rings.

The behavior of the mobility coefficient *D* of the Li atoms in the SP in the processes of intercalation and deintercalation is unpredictable (Fig. 4). The common feature of the behavior of *D* in all the considered cases is its high values during the initial period of intercalation. This is natural because, in the case of a small number of Li atoms in the pore, they are imparted with a higher specific value of the momentum from the Li^+ ions, which leads to the increase in the value of coefficient *D*. However, when the number of Li atoms in the SP exceeds 20, the relief of the pore walls starts strongly affecting the mobility of the Li atoms. Relative to this, the value of *D* can both decrease in the presence of monovacancies (Fig. 4b) and increase in the case of bivacancies (Fig. 4c). Also, coefficient *D* behaves unpredictably upon deintercalation. This value is subjected to sharp (for perfect silicene (Fig. 4a)) and long-term (for silicene with monovacancies) changes during delithization. The values of *D* may also decrease upon deintercalation by means of fluctuations in the same way that it takes place in the presence of bivacancies in silicene or almost continuously when trivacancies are present in silicene (Fig. 4d). In the case of

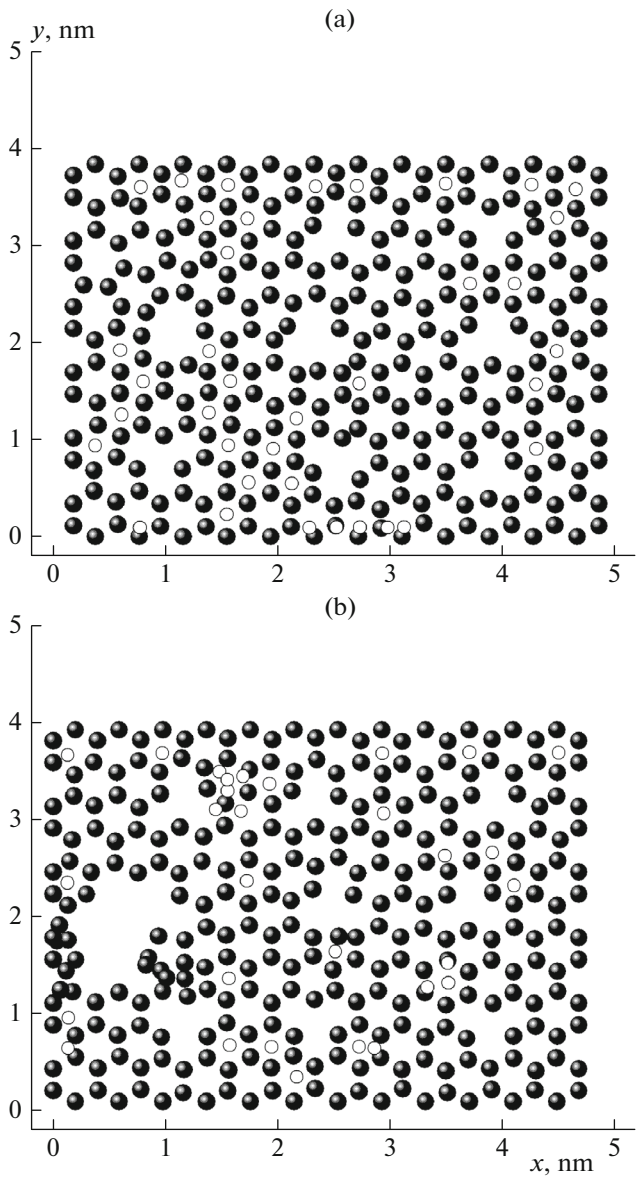

Fig. 3. *Xy* projections of the (a) upper and (b) lower silicene sheets with monovacancies on a Cu(111) substrate at the moment of full lithization (67 lithium atoms are present in the pore): (●) Si atoms and (○) Li atoms.

silicene with trivacancies, quite a strong rearrangement of the structure is observed in both silicene sheets. However, some defects retain their form in the upper sheet. The vertical distortion of the sheets after the process of lithization/delithization is not as significant.

For both perfect and defective silicene, the stresses σ_{zx} and σ_{zy} related to the introduction of lithium ions (atoms) into the SP are noticeably inferior to the stresses σ_{zz} which appear in the pore walls. Figure 5 shows the distributions of the average σ_{zx} and σ_{zz} stresses for the (*1*) upper and (*2*) lower silicene sheets

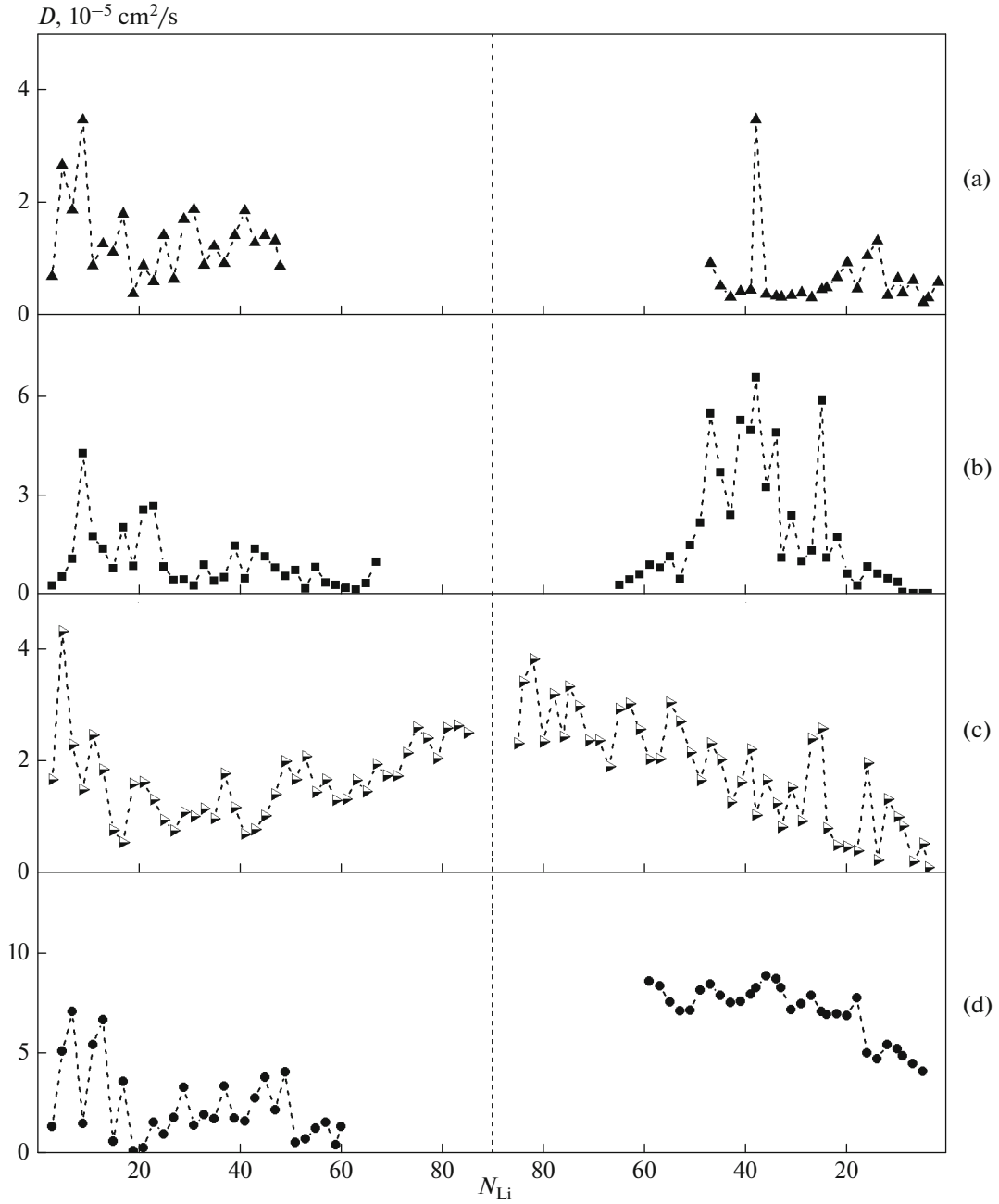

Fig. 4. Dependence of the mobility coefficient of lithium atoms D in the process of intercalation (to the left) and deintercalation (to the right) in silicene SPs with (a) perfect silicene and (b–d) silicene with (b) mono-, (c) bi-, and (d) trivacancie—on the number of lithium atoms N_{Li}.

obtained in the case of the SP being completely filled with lithium. These distributions are related to the case when the division of the sheets into surface elements moved forward along direction x ("zig-zag"), while the surface elements themselves are extended along direction y ("chair"). In the case of such a division, the strongest stresses σ_{zz} are obtained which are determined by the intercalation of lithium into the SP. These stresses are induced by the vertical strengths. As is seen from Fig. 5, strong local stresses σ_{zz} appear in the sheets of (a) perfect silicene as well as silicene with (c) bivacancies and (d) trivacancies upon the intercalation of lithium. The distributions of the stresses in the silicene sheets with (e) hexavacancies are overall similar to the corresponding distributions in the sheets with trivacancies (they are not shown in Fig. 5). The stresses σ_{zz} remain more significant in the silicene sheets with bivacancies upon deintercalation. The

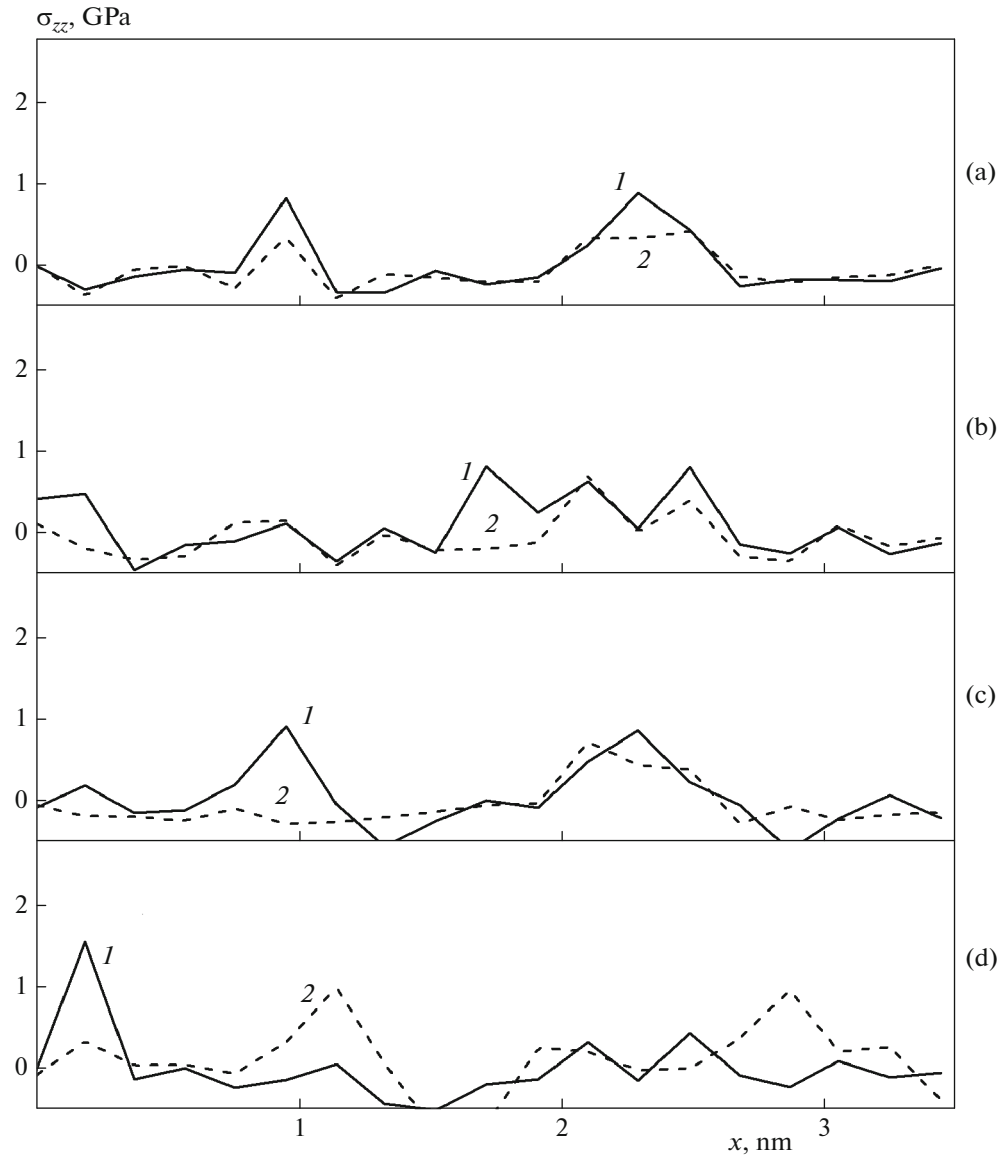

Fig. 5. Distribution of the σ_{zz} stresses in the silicene sheets forming a flat SP located on a Cu(111) substrate when the pore is filled with lithium to the limit depending on the type of the defects: (a) perfect silicene, (b) mono-, (c) bi-, and (d) trivacancies; N_{Li} = 48, 67, 86, and 60 (top to bottom).

maximum values of σ_{zz} achieved upon intercalation are approximately 17–19% of the ultimate tensile stress of silicene (20.45 GPa) [31] and are not critical.

CONCLUSIONS

According to the calculations, the silicene used in lithium-ion batteries should have defects only in the form of mono- and bivacancies. The application of perfect silicene and a silicene structure with such defects increases the number of adsorbed Li atoms by 20% on average in comparison with the case of the use of a silver substrate for supporting the silicene. The application of silicene with defects in the form of tri- and hexavacancies located on a copper substrate as an anodic material leads not only to the reduction (in relation to the small-size vacancy defects) of the number of adsorbed Li atoms but also to the destruction of the material of the anode.

During a real physical experiment, it is much easier to obtain a defective two-dimensional structure than a perfect one. Uncontrolled defects can be spontaneously formed. The formation of vacancies of a certain size can be controlled by scanning probe lithography [32] or ion bombardment [33, 34]. In the first case, a two-dimensional structure can be modified quite accurately. In the second case, the diameter of the scanning region is generally only several nanome-

ters, which makes it possible to quickly scan the surface and correct the size of the vacancies. Mono- and bivacancies are energy favorable defects and can be stable at quite high temperatures [35].

Lithium ions and atoms intercalated into a perfect silicene SP and a pore with mono- or bivacancies located on a copper substrate have approximately the same rate of diffusion. The rate of diffusion increases by more than an order of magnitude in the case of the use of silicene with tri- and hexavacancies. However, the instability of such a silicene structure does not make it possible to use this advantage. The preferable arrangement of an Li atom in a silicene pore is the position located over the center of a hexagonal Si ring. At the edges of the silicene sheets, the Li atoms are predominantly located over (or under) the Si atoms. The stresses σ_{zz} acting in the plane of the silicene sheets and induced by the interatomic interaction forces directed perpendicularly to these planes are predominant upon the intercalation of lithium into the pore. The stressed state of the walls of a silicene SP is not uniform; as a result of the movement of lithium atoms and ions in the pore, surges of the stress, the value of which does not exceed 19% of the ultimate tensile stress of silicene, occur.

FUNDING

This research was financially supported by the Russian Science Foundation (project no. 16-13-00061).

REFERENCES

1. A. E. Galashev and Yu. P. Zaikov, Russ. J. Phys. Chem. A **89**, 2243 (2015). https://doi.org/10.1134/S0036024415120122
2. A. E. Galashev and Yu. P. Zaikov, Russ. J. Electrochem. **51**, 867 (2015). https://doi.org/10.1134/S1023193515090050
3. A. E. Galashev and O. R. Rakhmanova, High Temp. **54**, 11 (2016). https://doi.org/10.1134/S0018151X15050120
4. A. E. Galashev, Yu. P. Zaikov, and R. G. Vladykin, Russ. J. Electrochem. **52**, 966 (2016). https://doi.org/10.1134/S1023193516100049
5. M. Kuhne, F. Paolucci, J. Popovic, P. M. Ostrovsky, J. Maier, and J. H. Smet, Nat. Nanotech. **12**, 895 (2017). https://doi.org/10.1038/nnano.2017.108
6. O. R. Rakhmanova and A. E. Galashev, Russ. J. Phys. Chem. A **91**, 921 (2017). https://doi.org/10.1134/S003602441705020X
7. A. E. Galashev, K. A. Ivanichkina, A. S. Vorob'ev, and O. R. Rakhmanova, Phys. Solid State **59**, 1242 (2017). https://doi.org/10.1134/S1063783417060087
8. A. Y. Galashev and K. A. Ivanichkina, Phys. Lett. A **381**, 3079 (2017). https://doi.org/10.1016/j.physleta.2017.07.040
9. A. E. Galashev and K. A. Ivanichkina, Russ. J. Phys. Chem. A **91**, 2448 (2017). https://doi.org/10.1134/S003602441712007X
10. H. Sitinamaluwa, J. Nerkar, M. Wang, S. Zhang, and C. Yan, RSC Adv. **7**, 13487 (2017). https://doi.org/10.1039/C7RA01399J
11. G. A. Tritsaris, E. Kaxiras, S. Meng, and E. Wang, Nano Lett. **13**, 2258 (2013). https://doi.org/10.1021/nl400830u
12. R. Quhe, Y. Yuan, J. Zheng, et al., Sci. Rep. **4**, 5476 (2014). https://doi.org/10.1038/srep05476
13. S. Cahangirov, V. O. Ozcelik, L. Xian, et al., Phys. Rev. B **90**, 035448 (2014). https://doi.org/10.1103/PhysRevB.90.035448
14. L. Chen, H. Li, B. Feng, et al., Phys. Rev. Lett. **110**, 085504 (2013). https://doi.org/10.1103/PhysRevLett.110.085504
15. J. Echigoya, H. Enoki, T. Satoh, et al., Appl. Surf. Sci. **56**, 463 (1992). https://doi.org/10.1016/0169-4332(92)90272-Y
16. J. Zhang, C. Liu, Y. Shu, and J. Fan, Appl. Surf. Sci. **261**, 690 (2012). https://doi.org/10.1016/j.apsusc.2012.08.082
17. C. A. F. Vaz, S. J. Steinmuller, C. Moutafis, J. A. C. Bland, and A. Y. Babkevich, Surf. Sci. **601**, 1377 (2007). https://doi.org/10.1016/j.susc.2007.01.001
18. J. Tersoff, Phys. Rev. B **38**, 9902 (1988). https://doi.org/10.1103/PhysRevB.38.9902
19. J. Tersoff, Phys. Rev. B **49**, 16349 (1994). https://doi.org/10.1103/PhysRevB.49.16349
20. S. M. Foiles, M. I. Baskes, and M. S. Daw, Phys. Rev. B **33**, 7983 (1986). https://doi.org/10.1103/PhysRevB.33.7983
21. R. Yu, P. Zhai, G. Li, and L. Liu, J. Electron. Mater. **41**, 1465 (2012). https://doi.org/10.1007/s11664-012-1916-x
22. S. K. Das, D. Roy, and S. Sengupta, J. Phys. F: Metal. Phys. **7**, 5 (1977). https://doi.org/10.1088/0305-4608/7/1/011
23. T.-E. Fang and J.-H. Wu, Comp. Mater. Sci. **43**, 785 (2008). https://doi.org/10.1016/j.commatsci.2008.01.066
24. Y. Pan, L. Zhang, L. Huang, et al., Small **10**, 2215 (2014). https://doi.org/10.1002/smll.201303698
25. G. R. Berdiyorov, H. Bahlouli, and F. M. Peeters, J. Appl. Phys. **117**, 225101 (2015). https://doi.org/10.1063/1.4921877
26. K. Kawahara, T. Shirasawa, R. Arafune, et al., Surf. Sci. **623**, 25 (2014). https://doi.org/10.1016/j.susc.2013.12.013
27. G. R. Berdiyorov, M. Neek-Amal, F. M. Peeters, and A. C. T. van Duin, Phys. Rev. B **89**, 024107 (2014). https://doi.org/10.1103/PhysRevB.89.024107
28. A. Y. Galashev and K. A. Ivanichkina, J. Electrochem. Soc. **165**, A1788 (2018). https://doi.org/10.1149/2.0751809jes

29. S. Plimpton, J. Comp. Phys. **117**, 1 (1995). https://doi.org/10.1006/jcph.1995.1039
30. A. E. Galashev, Phys. Met. Metallogr. **117**, 238 (2016).
31. R. E. Roman and S. W. Cranford, Comp. Mater. Sci. **82**, 50 (2014). https://doi.org/10.1016/j.commatsci.2013.09.030
32. S. Neubeck, F. Freitag, R. Yang, and K. S. Novoselov, Phys. Status Solidi B **247**, 2904 (2010). https://doi.org/10.1002/pssb.201000186
33. L. Tapaszto, G. Dobrik, P. Nemes-Incze, G. Vertesy, Ph. Lambin, and L. P. Biro, Phys. Rev. B **78**, 233407 (2008). https://doi.org/10.1103/PhysRevB.78.233407
34. Y. Kowaki, A. Harada, F. Shimojo, and K. Hoshino, J. Phys.: Condens. Matter **21**, 064202 (2009). https://doi.org/10.1088/0953-8984/21/6/064202
35. A. E. Galashev and O. R. Rakhmanova, Phys. Usp. **57**, 970 (2014). https://doi.org/10.3367/UFNe.0184.201410c.1045

Translated by E. Boltukhina